A Novel Approach for Nonlinear Distortion Correction of Industrial Endoscope Images

Hui-xian SUN [1], Yu-hua ZHANG [1], Fei-lu LUO [1]

[1]National University of Defense Technology; Changsha, China
Phone: +86 0731 4574994; e-mail: sunhuixian@nudt.edu.cn, zhangyuhua@nudt.edu.cn

Abstract: Industrial endoscopes inspection is an important method of remote visual testing. The endoscope image suffers from a nonlinear spatial distortion due to the wide-angle design of the endoscope's objective lens. The spatial distortion causes the pixels shift, which makes the object distorted in an image. By correcting the pixel's offset in Cartesian coordinate, a novel approach for nonlinear distortion correction of industrial endoscope images is proposed in this paper. Based on a dot array calibration template correction method, cubic B-spline interpolating function is adopted to interpolate the curved faces of the pixel's offset in X- and Y- axis separately. As a result, the offsets of each pixel are obtained in the distorted image. Furthermore, the pixels shift is rectified to achieve an undistorted image by coordinate conversion. A modified bilinear interpolation is used to evaluate the gray level of pixels, which is not assigned in coordinate conversion. The proposed method is applied to several endoscope images. The results show that the proposed method can correct the nonlinear distortion of endoscope images effectively.

Keywords: industrial endoscope; nonlinear distortion correction; cubic spine interpolating function; curve face

1. Introduction

Visual inspection is one of the most basic Nondestructive Testing methods. As an important equipment of visual inspection, industrial endoscope is widely applied to internal structural inspections in aircraft maintenance, power stations inspections, automotive repair, etc. However, endoscope images suffer from barrel-type spatial distortion due to the wide-angle design of the endoscope objective lens[1]. The distortion introduces nonlinear changes in the image. In the distorted images, areas near the distortion center are compressed less, while areas farther from the center are compressed more. As a result, the outer areas of the image look significantly smaller than their actual size. So, nonlinear distortion correction of endoscope images is very important for practical inspection.

In recent years, several methods have been presented for the nonlinear distortion correction[2-5]. In these methods, only radial distortion is considered, because an ideal endoscope lens is circularly symmetric. Generally, a calibration template is used to provide distortion image. Firstly, the image is transformed from 2D Cartesian coordinate to polar coordinates. Because of radial distortion, every pixel's distortion is decided by the distance of the pixel to optical center and unrelated with angle value. Thus it is very important to estimate the optical center of endoscope. As is often the case that the parameters of endoscope optical system is unknown and the optical measurement equipment is unattainable. Consequently, it is difficult to estimate the optical center of endoscope accurately. In the actual correction, the distortion center of the distorted image is treated as optical center[6, 7]. So the optical center estimate error becomes one of the main errors of distortion correction.

In this paper, a novel method for distortion correction of endoscope images is proposed based on distortion curved face interpolation. A standard dot array calibration template comes into use for correcting the pixel's offset in Cartesian coordinate. The cubic B-spline interpolating function is adopted to interpolate the curved faces of the pixel's offset in X- and Y- axis separately. The offsets of each pixel are obtained in the distorted image. Furthermore, the pixels shift is rectified to achieve an undistorted image by coordinate

conversion. A modified bilinear interpolation is used to evaluate the gray level of pixels, which is not assigned in coordinate conversion. The proposed method is applied to correct the nonlinear distortion of several endoscope images successfully.

2. Distortion and Correction Theory

2.1 Endoscope Image Distortion

Based on geometry optics theory, an ideal image can form in an optical system when the object is in the paraxial region. But the viewing region is larger than the paraxial region in an actual optical. Thus, there is aberration between ideal image and actual image in position and size. The endoscope image distortion is one of optical aberrations. Figure 1 shows two typical distortion models of optical system. Figure 1(a) is original standard grid, Figure 1(b) and Figure 1(c) are respectively pillow-type distortion and barrel-type distortion. In pillow-type distortion image, areas near the distortion center are compressed more, while areas farther from the center are compressed less. In barrel-type distortion image, the situation of distortion is just the contrary. The distortion of endoscope images is a typical barrel-type spatial distortion[8].

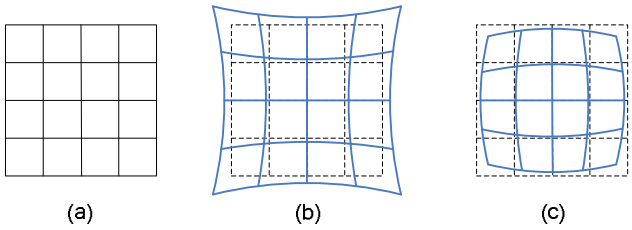

Figure1. Distortion model of optical system. (a) Original grid. (b) pillow-type distortion. (c) barrel-type distortion

2.2 Correction Theory

In endoscope image, the spatial distortion causes the pixels shift, which makes the object distorted. The spatial distortion correction using digital image processing is actually to restore the distorted image.

The relation of coordinates between the ideal image $f(u, v)$ and distorted image $f(x, y)$ could be expressed:

$$(x, y) = T_a[(u, v)] \quad (1)$$

Where, T_a is a non-linear transform.

Essentially, a digital image is a 2D array of intensity or chromaticity. The spatial distortion can be equivalent to the pixel's offset. Moreover, these offset can be decomposed in X- and Y- axis separately in Cartesian coordinate. Each pixel $f_p(x_p, y_p)$ in endoscope image has a corresponding pixel $f_p(u_p, v_p)$ in ideal image, and they can transform reciprocally.

$$\begin{cases} u_p - \Delta x = x_p \\ v_p - \Delta y = y_p \end{cases} \quad (2)$$

Where, Δx and Δy are offsets of pixel in X- and Y- axis.

According to geometry optics theory, the offsets of image point in image plane are continuous. So, in digital image every pixel offset in X- axis compose a curve, either in Y- axis. If the two curves can be obtained, offsets (Δx and Δy) of every pixel in endoscope image are obtained. Then, the distortion correction of endoscope image can be realized.

3. Correction Method and Its Realization

3.1 Calibration Template

The dot array calibration template is shown in Figure 2. In the template, dots array in-line square pitch,

and each dot has the same distance with its four adjacent dots.

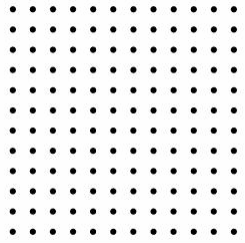

Figure 2. Dot array calibration template

3.2 Fixing of Round Spot Centers

(1) Pro-processing for template image

Pro-processing for template image is consisted of image enhancement, image binarizing, and median filtering. To enhance image contrast, image subtraction is adopted between the original image and the image after lowpass filtering. This method is simple and can eliminate effect of light intensity variant. Because the original calibration dot pattern has basically ideal black-and-white contrast, the image binarizing can be realized by one threshold. The final result is obtained by applying a median filter to remove any extraneous salt and pepper noise.

(2) Dot Centroid Estimation

The next step of processing is to estimate the center of dots. Due to distortion, the figures of dots are different to ideal round spot. Generally, center of deformed solid circle can be replaced by its centroid. The centroid (x_c^i, y_c^i) for dot c is calculated using the N_i pixels making up dot i.

$$\begin{cases} x_c^i = = \dfrac{1}{N_i}\sum_{k=1}^{N_i} x_k^i \\ y_c^i = = \dfrac{1}{N_i}\sum_{k=1}^{N_i} y_k^i \end{cases} \quad (3)$$

3.3 Distortion Curved Face Interpolation

According to the analysis of endoscope image distortion and correction theory in Section 2, it is indicated that if the two curve faces of offsets in X- and Y- axis are obtained, the spatial distortion can be corrected. The positions of dots in distorted image have been fixed in operation above. At the some time, the positions of dots in ideal image must be estimated to interpolate the curves. A dot of the distorted image must be specified, which is the corresponding one in ideal image, and the distance of two adjacent dots is estimated. Because of regular array of dots, an ideal dot array image can be obtained.

The distances of every dot and its four adjacent dots are calculated, and their sum is $\sum L_i$. The dot is specified the corresponding dot, which distance sum is the maximum. Figure 3 shows that dot A is the corresponding dot, and the sum of distances with four adjacent dots is $\sum L_A$.

$$\Sigma \mathrm{L}_A = X_{AB} + X_{AD} + Y_{AC} + Y_{AE} \quad (4)$$

Where, X_{AB}=□x_A-x_B□, x_A, x_B respectively represent the value of dot A and dot B in X- axis. X_{AB} is the distance between dot A and dot B in X- axis. In the same way, X_{AD} is the distance between dot A and dot D in X- axis, and Y_{AC}, Y_{AE} are respectively the distance between dot A and dot C, E in Y- axis.

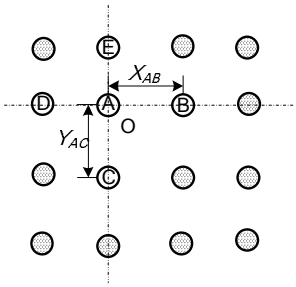

Figure 3. Dot position of the calibration template image

The distance D of two adjacent dots is calculated as

$$D = (1+\alpha+\beta)\cdot D' \qquad (5)$$

Where, $D' = \max\{X', Y'\}$, $X' = \max\{X_{AB}, X_{AD}\}$, $Y' = \max\{Y_{AC}, Y_{AE}\}$, $\alpha = \dfrac{|X_{AB} - X_{AD}|}{X'}$

$\beta = \dfrac{|Y_{AC} - Y_{AE}|}{Y'}$.

Then, the offsets of each dot center are obtained. Figure 4 shows the mesh figure of offsets in X- and Y- axis respectively.

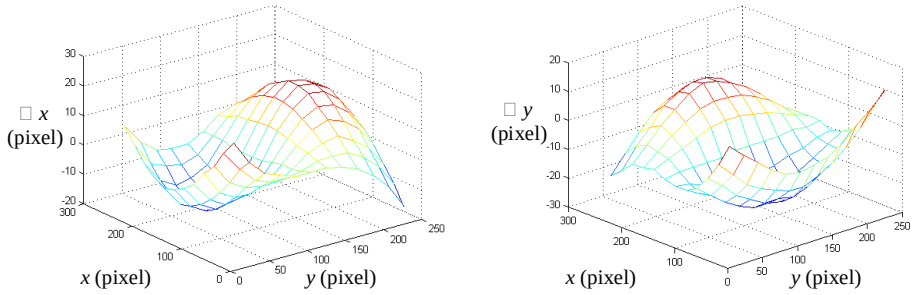

(a) (b)

Figure 4. Offset of dots in distorted calibration template image. (a) Offset in X-axis. (b) Offset in Y- axis.

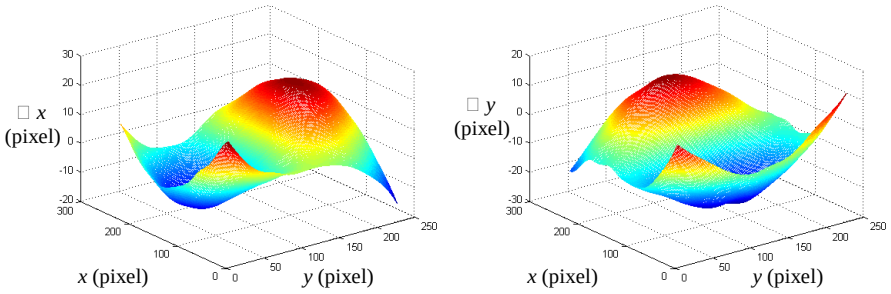

(a) (b)

Figure 5. Curved face of pixel's offset after cubic B-spline interpolation. (a) Offset in X-axis. (b) Offset in Y- axis.

To construct the curve face of all pixels offsets in distorted image, cubic B-spline function is selected to interpolate the curve faces in X- and Y- axis. Two steps are needed to interpolate the curve face. The first step is to obtain curves family in X- (or Y) axis using interpolation method. The second step is to interpolate points on curve face in Y- (or X) axis. Although the order of B-spline increases with the increase of primary function order, the merits of B-spline are preserved. The smoothness of B-spline is increased as its order increased. But the calculating amount is increased rapidly. The curve interpolating by cubic B-spline function can realize second-order continuity and meet requirement of most engineering. Figure 5

shows the curved faces of pixel's offset after cubic B-spline interpolation.

3.4 Conversion of Coordinates

The goal of conversion of coordinates is to rectify the pixels offsets to achieve an undistorted image based on curved faces of pixel's offset. The relationship of pixel $f_p(x_p, y_p)$ in endoscope image and pixel $f_c(x_c, y_c)$ in corrected image are calculated as follows:

$$\begin{cases} x_p + \Delta x = x_c' \\ y_p + \Delta y = y_c' \end{cases}, \quad (6)$$

Where, Δx_p and Δy_p are offsets of pixel in endoscope image in X- and Y- axis, which is obtained from the curved faces of pixel's offset. (x_c, y_c) is the round of (x'_c, y'_c).

3.5 Bilinear Interpolation

After conversion of coordinates, each pixel of distorted image has been filled in corrected image. But the actual distorted image is smaller than the ideal image because of barrel-type distortion. So some pixels are not assigned a value in corrected image. The bilinear interpolation method is selected to evaluate the gray level of the pixels. Considering the practical situation, a modified bilinear interpolation is employed.

$$f(x, y) = \frac{1}{4}[a + b + c + d] \quad (8)$$

Where, $f(x, y)$ is the pixel to interpolate, $a=f(x, y-1)$, $b=f(x, y+1)$, $c=f(x-1, y)$, $d=f(x+1, y)$. Furthermore, the adjacent pixel of $f(x, y)$ has not been assigned possibly. For example, $f(x, y-1)$ has not assigned, then $a=f(x, y-2)$. If $f(x, y-2)$has not been assigned, then $a=f(x, y-2)$,... The evaluation of b, c, d are the same as a.

4. Experiment

The Dot array calibration template is shown in Figure 1. The diameter of dot is 1mm, and the distance between the centers of two adjacent dots is 2.5mm. The endoscope is vertically placed before the template with their distance is 70mm. Figure 6 shows image of the calibration template. Figure 6(a) shows the original input video image digitized directly from the endoscope. It is obvious that the barrel-type distortion exists in the image. Figure 6(b) shows the results of a distortion correction using the proposed method. The spacing distances of dots are homogeneous, and the dots array regularly. The nonlinear distortion of endoscope images can be correct by the proposed method effectively.

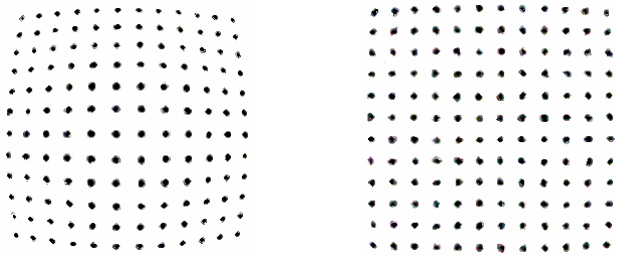

(a) (b)

Figure 6. Image of the calibration template, (a) Distorted image. (b) Corrected image.

To analysis the correct result quantitatively, three errors are defined based on distorted template image and the corrected one. It is noticed that the sizes of two images are different and they are not in the same coordinate plane. The dot, which sum of distances with four adjacent dots is maximal, is selected as the reference dot O.

(1) Horizontal-direction error E_x

$$E_x = | X_{OA} - X'_{OA} | \quad (7)$$

Where, X_{OA} are distances between reference dot *O* and the other dot in X- axis in the ideal template image. X'_{OA} are the distances in the distorted image or the corrected image.

(2) Vertical-direction error E_y

$$E_y = | Y_{OA} - Y'_{OA} | \tag{8}$$

It is the same as Horizontal-direction offset that Y_{OA} and Y'_{OA} are distance between the two dots in Y-axis.

(3) Euclidean-distance error E_{xy}

$$E_{xy} = | d_{OA} - d'_{OA} | \tag{9}$$

It is the same as Horizontal-direction offset that d_{OA} and d'_{OA} are the Euclidean-distance between the two dots.

The maximum and average values of there errors are computed over all dots. The results are shown in Table1. The distortion of template image is obvious before correction. The maximal offset in horizontal direction or vertical direction reach 14 pixels and the average values of three type errors are all greater than 1 pixel. But after correction by the proposed method, the average values are all less than 1 pixel. To demonstrate the effect of the proposed method, several images are captured and corrected by the same correction model. Two typical images are shown in Figure7. It can be noted that in the original images areas near the distortion center are compressed less, while areas farther from the center are compressed more. But the corrected images are quit favorable for the visual observation.

Table 1. Error of dots in the calibration template image

Error	Error type	Before correction	After correction
E_x (pixel)	maximum	14	3
	average	4.48	0.47
E_y (pixel)	maximum	14	3
	average	4.52	0.48
E_{xy} (pixel)	maximum	16.64	3.25
	average	6.26	0.57

(a) (b) (c) (d)

Figure 7. Experimental images. (a) Distorted image A. (b) Corrected image A.
(c) Distorted image B. (d) Corrected image B.

5. Conclusion

In this paper, a novel approach for nonlinear distortion correction of industrial endoscope images based on distortion curved face interpolation is proposed. The results show that the method for distortion correction is validity. The method is easy to implement, and does not need to solve equations. At the same time, the correction precision in the whole image is not affected by estimation error of distortion center. The method can correct the radial spatial distortion of wide-angle objective lens effectively. Moreover, it

can be generalization to correct other spatial distortion of optical system.

Reference

[1] PAUL E. MIX. Introduction to Nondestructive Testing: A Training Guide[M]. 2nd ed. New York: John Wiley & Sons, Inc. 2005.

[2] SMITH E, VAKIL N, MAISLIN S A. Correction of distortion in endoscope images[J]. IEEE Transactions on Medical Imaging, 1992, 11(1): 117-122.

[3] HIDEAKI H, YUTAKA Y, YOICHI M. A new method for distortion correction of electroinic endoscope images[J]. IEEE Transactions on Medical Imaging, 1995, 14(3): 548-555.

[4] STEFANSIC J D, HERLINE A J, CHAPMAN W C, et al. Endoscopic tracking for use in interactive image-guided surgery[C]. Proceeding of SPIE, San Diego, California, 1998.

[5] ASARI K V, KUMAR S, RADHAKRISHNAN D. A new approach for nonlinear distortion correction in endoscopic images based on least squares estimation[J]. IEEE Transactions on Medical Imaging, 1999, 18(4): 345-354.

[6] LIU H, YU D Y, DU J, et al. Distortion correction of the wide-angle optical system with digital technology[J]. Acta Optica Sinica,1998, 18(8): 1108-1112.

[7] Xie H B, CHEN D Q, YU D Y. Study on correction of distortion in medical electronic endoscope image[J]. Proceeding of SPIE, Aaron Fenster, 2001.

[8] HELFERTY J P, ZHANG C, MCLENNAN G, et al. Videoendoscopic distortion correction and its application to virtual guidance of endoscopy[J]. IEEE Transactions on Medical Imaging, 2001, 20(7): 605-617.